Crystallization on prestructured seeds

Swetlana Jungblut and Christoph Dellago
Faculty of Physics, University of Vienna, Boltzmanngasse 5, 1090 Wien, Austria
(Received 7 November 2012; published 10 January 2013)

The crystallization transition of an undercooled monodisperse Lennard-Jones fluid in the presence of small prestructured seeds is studied with transition path sampling combined with molecular dynamics simulations. Compared to the homogeneous crystallization, clusters of a few particles arranged into a face- and body-centered cubic structure enhance the crystallization, while icosahedrally ordered seeds do not change the reaction rate. We identify two distinct nucleation regimes—close to the seed and in the bulk. Crystallites form close to the face- and body-centered structures and tend to stay away from the icosahedrally ordered seeds.

DOI: 10.1103/PhysRevE.87.012305 PACS number(s): 64.70.D−, 64.60.qe, 64.75.Gh

I. INTRODUCTION

As has been known for more than 100 years, the presence of impurities can strongly enhance crystallization of undercooled fluids [1]. Such seeded crystallization provides a way to control the crystallization kinetics and influence the micromorphology of the target crystalline material [2,3]. Recent experiments on colloidal systems [4] and computer simulations of hard spheres [5] showed that a simple spherical impurity indeed acts as a crystallization site, but only if the sphere is comparatively large. On the other hand, for a two-dimensional Ising system the presence of a single fixed spin dramatically increases the nucleation rate [6]. In addition, most impurities are more complicated than a single sphere, and of particular interest are crystallization sites made of the same species as the crystallizing substance. Thus, several experimental and theoretical studies were dedicated to the studies of crystallization on prestructured clusters and surfaces [2,3,7–14]. It was shown that two-dimensional (flat) patterned templates influence the structures of the crystals growing in three-dimensional undercooled fluids [2,9]. Other simulations [10] considered the effect of the lattice constant of the template and found that the crystals attach to the template and grow only in one direction in the incommensurate case, and respectively, are symmetrical around the template in the commensurate case. Recently [15], we considered crystallization on small three-dimensional clusters with a lattice constant smaller than the bulk constant of the crystal and a diameter smaller than the threshold at which the simple spheres will induce crystallization [4,5]. We showed, for seeds of the same size, that the structure of the seeds determines whether their presence will enhance crystallization or not.

In this paper, we present results on the crystallization of a supercooled liquid in the presence of the prestructured clusters with the lattice spacing of the bulk crystals and the smallest possible sizes that can still be assigned to particular lattice structures. We show, using transition path sampling simulations combined with committor analysis of the transition mechanism, that the effect on the transition rate is determined by the structure of the seed. While seeds with structures similar to the bulk crystal such as face-centered cubic (fcc) and body-centered cubic (bcc) enhance crystallization by several orders of magnitude, the presence of completely incommensurate icosahedral seeds has no effect on the crystallization transition. The latter result is in contrast to previous simulations [15], in which icosahedral seeds with smaller lattice spacing were observed to influence the transition pathway but not the transition rate. In the early crystallization stages, crystals around a bcc seed were found to grow at a higher rate than those around an fcc seed, an example of Ostwald's step rule. This effect, however, reverses in later crystallization stages leading to the overall higher increase of the crystallization rate by an fcc seed.

The remainder of the paper is organized as follows. In Sec. II, we provide details about the simulation methods used in our study. Results on the kinetics and the mechanism of the crystallization transition are presented and discussed in Sec. III. A brief summary is given in Sec. IV.

II. SIMULATION DETAILS

We perform molecular dynamics (MD) simulations of a system of particles interacting via the truncated and shifted Lennard-Jones (LJ) potential with the cutoff distance of $r_c = 2.5$. Here, we use LJ units throughout the paper. We integrate the system at constant pressure and constant enthalpy (NpH ensemble [16]) with a time step of $\Delta t = 0.01$. The pressure is set to $p = 0.003\,257$ and the enthalpy per particle such that the initial temperature of the undercooled fluid is $T = 0.527$, which corresponds to $\sim 25\%$ undercooling. The initial cooling and equilibration are performed by periodically rescaling the particle velocities to achieve the desired temperature (NpT ensemble). The obtained configurations are then used to simulate the crystallization of a homogeneous system with $N = 6668$ particles. For the simulations of heterogeneous crystallization, a seed is inserted into the system and the configuration is then equilibrated for another 2×10^5 time steps. Our heterogeneous systems contain $N = 6617$ particles which are allowed to move freely and either $N_{\mathrm{fcc/icos}} = 13$ (to form fcc and icosahedral seeds) or $N_{\mathrm{bcc}} = 15$ (to reproduce a bcc structure) fixed particles. The lattice constant of all seed structures is set to 1.09. Thus, the outer particles in fcc and icosahedral seeds are at a distance of 1.09 from the central particle. In the bcc structure, eight particles in the first shell are at 1.09 and six particles in the second shell are at 1.26 from the central one. Minimum image periodic boundary conditions apply in all directions.

As an order parameter of the crystallization process, we use the number of particles in the largest crystalline cluster, n_s. The clusters are identified following the scheme proposed

by Auer and Frenkel [17], which is based on Steinhardt bond order parameters [18], which analyze structural correlations in the surroundings of a particle. Within this scheme, if only seed particles are taken into account, the central particles of fcc and bcc seeds are identified as solid, while all particles in the icosahedral as well as all outer particles in the cubic seeds are considered liquid.

We also use a combination of averaged Steinhardt bond order parameters [19] to distinguish between particles in the fcc, hcp, icosahedral (fivefold symmetric), bcc, and distorted bcc environments [20]. The last structure corresponds to the $I\bar{4}3d$ phase recently discovered in a LJ system [21].

Another combination of Steinhardt bond order parameters, recently put forward by Kawasaki and Onuki [22], allows one to evaluate the surrounding structures in terms of the deviation from hexagonal ordering, thus measuring the disorder of crystalline structures.

We perform transition interface sampling (TIS) [23] simulations to sample trajectories that connect the supercooled liquid to the crystalline phase. The number of attempted moves, which include 90% shooting and 10% path reversal moves, is at least 10^3 for equilibration and 10^4 for sampling. In shooting moves, the amplitude of the velocity change distribution is adjusted to keep the acceptance probability between 20% and 30%. The interval between two configurations along a particular path that are used as shooting points is $\Delta t = 0.1$. We set the interfaces for the TIS simulations such that the probability to reach the next window is at least about 10%. To obtain this minimum crossing probability, we use different definitions of the interfaces in various cases. For all simulations, the initial undercooled state includes all configurations with the largest clusters smaller than $n_s = 20$ particles, the first interface is placed at $n_s = 30$ particles, and the region in-between is used to calculate the flux through the first interface. The positions of the remaining interfaces are $n_s = 50,80,110,140,170,230,300,400$ for the simulations without a seed, $n_s = 50,80,110,150,190,230,300,400$ for the simulations with icosahedral seeds, and $n_s = 50,80,120,170,230,300,400$ for the other seeds. The final state of the reaction is the fully crystallized system, however, we stop sampling when the crossing probability becomes constant, since all configurations containing crystalline clusters larger than, in our case, 400 particles always continue to evolve into crystallinity.

III. RESULTS AND DISCUSSION

A. Reaction rate

The most prominent effect of the presence of prestructured seeds is on the crystallization rate, J. We find the crystallization rate, i.e., the number of crystallization events per unit time and volume, from the product of the flux through the first interface, f_{first}, and the probability to reach the final state of reaction given that the system crossed the first interface, $P(n_{\text{last}}|n_{\text{first}})$:

$$J = \frac{f_{\text{first}}}{V} P(n_{\text{last}}|n_{\text{first}}), \tag{1}$$

TABLE I. Flux through the first interface, f_{first}, average simulation box volume, V, crossing probability to reach the last interface, $P(n_{\text{last}}|n_{\text{first}})$, and the crystallization rate, J, for systems with fcc, bcc, icosahedral seed, and without seed.

	fcc	bcc
f_{first}	0.49 ± 0.01	0.50 ± 0.01
V	7258.7 ± 0.1	7262.1 ± 0.1
f_{first}/V	$6.77 \pm 0.14 \times 10^{-5}$	$6.82 \pm 0.18 \times 10^{-5}$
$P(n_{\text{last}}\|n_{\text{first}})$	$1.1 \pm 0.2 \times 10^{-4}$	$1.1 \pm 0.3 \times 10^{-5}$
J	$7.6 \pm 1.5 \times 10^{-9}$	$7.3 \pm 1.7 \times 10^{-10}$
	icos	no seed
f_{first}	0.30 ± 0.01	0.30 ± 0.01
V	7259.0 ± 0.1	7301.7 ± 0.1
f_{first}/V	$4.15 \pm 0.15 \times 10^{-5}$	$4.10 \pm 0.13 \times 10^{-5}$
$P(n_{\text{last}}\|n_{\text{first}})$	$4.1 \pm 1.5 \times 10^{-8}$	$4.7 \pm 1.7 \times 10^{-8}$
J	$1.7 \pm 0.6 \times 10^{-12}$	$1.9 \pm 0.7 \times 10^{-12}$

where V is the average volume of the simulation box in the initial state. Table I contains the values of f_{first} and V calculated in a straightforward MD simulation of the initial phase.

The values of the box volume are comparable, although the presence of the bcc seed, which is larger than the other seeds, is slightly noticeable. The homogeneous box is also larger, since it contains more particles. Thus, we use the flux density f_{first}/V to compare the behavior of the initial phases of our systems.

The fluxes in the presence of cubic seeds are similar, the flux for fcc being marginally smaller, and larger than in the homogeneous case. In contrast, in the presence of an icosahedral seed the flux density is comparable to the homogeneous system. For small cluster sizes, the results for the crossing probabilities show the same tendency—as demonstrated in Fig. 1—it is more likely to reach a cluster size of up to about 150 particles in the presence of a bcc seed than in any other case. At later stages of the reaction, the crossing probability in the presence of an fcc seed prevails

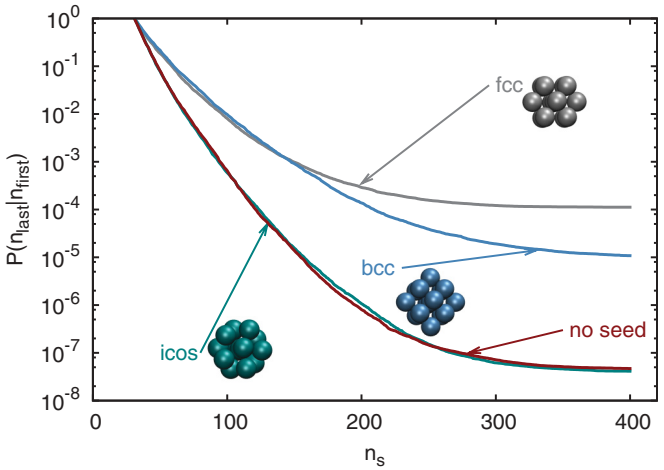

FIG. 1. (Color online) Conditional crossing probabilities $P(n_s|n_{\text{first}})$ obtained with TIS in the presence of fcc, bcc, icosahedral seeds, and in a homogeneous system as a function of the largest cluster size, n_s. The crossing probability for small clusters in the presence of a bcc seed is slightly higher than in the presence of an fcc seed.

over the crossing probability in the presence of a bcc seed. For the icosahedral seed, we find that the crossing probability follows the results of the homogeneous case. Altogether, the presence of an fcc seed increases the crossing probability, and, thus, the crystallization rate by more than three orders of magnitude. The effect of the bcc seed is smaller by about one order of magnitude, and the icosahedral seed does not change the reaction rate at all compared to the seedless case. In a previous work [15], we considered seeds with a lattice constant slightly smaller (1.0) than in equilibrium (1.09) and at undercooling of $\sim$28%, yielding a reaction rate increased by the presence of an fcc seed by one order of magnitude, while an icosahedrally structured seed had again no effect on the crystallization rate (but it affected the nucleation pathway as a considerable fraction of crystals nucleated on the seed surface). At this undercooling, the presence of an fcc seed with equilibrium lattice constant forces the system to crystallize too easily, thus, we went to higher temperatures for better statistics.

In this work, we also consider the effect of the presence of a bcc-structured seed. Although the overall results are unsurprising—since the bcc structure in equilibrium is close to the more stable fcc structure, while icosahedrally ordered crystals are energetically less stable—we expect the reaction rate in the presence of a bcc seed to lay somewhere between fcc and icosahedral rates. Indeed, that is where we find it. However, at small cluster sizes, the crossing probability is larger than for an fcc seed. This is an example of Ostwald's step rule [1,24], which states that the system evolution follows the route of the smaller free energy difference. In our case, the energy of the undercooled liquid is closer to that of the bcc crystals, which is not the equilibrium structure; thus, the fluid first prefers to form bcc-structured crystals, which transform into the more stable fcc phase only in later stages of the nucleation process. Hence, at the beginning of the reaction, the presence of a bcc seed enhances the formation of bcc clusters, but these clusters still have to rearrange into the fcc structure. The presence of an fcc seed supports the direct formation of fcc structures and the rearrangement step is omitted, thus, the probability to form larger crystallites is larger in systems with fcc seeds.

B. Structure of clusters

In the following, we study the details of the crystallization process considering a selection of 100 crystallizing paths connecting the initial undercooled liquid state ($n_s <$ 20) to the states with cluster sizes of more than 1000 particles.

From all configurations along these pathways, we extract the states with the same size of the largest cluster (in steps of five particles) and calculate the average fractions of particles in the icosahedral, fcc, hcp, bcc, and distorted bcc environments in the largest cluster and its core, which includes those particles in the cluster without liquid neighbors. The results are presented in Fig. 2. Since the fractions of icosahedral structures in the crystallites are very small for all types of seeds, they are not shown in the figure.

The presence of an icosahedral seed yields the same cluster structures as in the homogeneous case: The fraction of particles with fcc surroundings prevails over other structures and is larger in the core of the cluster than in the whole cluster. Furthermore, the fraction of hcp particles, which are mainly due to stacking faults, is smaller but grows steadily. Interestingly, icosahedral structures with fivefold symmetry can arise along the lines where two hcp stacking-fault planes (twinning planes) intersect at certain angles. These icosahedral structures, however, are rather rare with fractions below 1% in all cases. The fraction of bcc particles, which concentrate on the surface of the cluster, is large for smaller clusters and shrinks as the clusters become larger, reflecting the decreasing surface to volume ratio of the growing crystallite. Such behavior is another confirmation of Ostwald's step rule [1,24], as, on average, the fluid particles first freeze into bcc and distorted bcc and only then rearrange into fcc and hcp structures.

The presence of cubic seeds modifies mostly the fractions of fcc, hcp, and bcc structures. In a system with an fcc seed, we find the cores of the small clusters being almost all fcc, while the fraction of bcc structures is depleted. However, larger clusters recover the compositions of the homogeneous case. For a bcc seed, the effect for small clusters is reversed—there are more bcc and less fcc structures, while the larger clusters are once more similar to the homogeneous system. The fraction of hcp structures in the clusters and their cores is slightly depleted in both cases, somewhat larger in the bcc case. Obviously, the seeds are too small to influence the larger clusters. Nonetheless, small crystallites are formed according to the introduced seed pattern unless the seed is icosahedral, for which the homogeneous result is recovered for all cluster sizes.

An explanation for this observation can be found in Fig. 3, where the attachment of the crystalline clusters to the seed is shown. For the icosahedral seed, the crystal formed somewhere in the bulk away from the seed in all cases but one. In contrast, fcc and bcc seeds are mostly either partially or entirely covered by the crystalline particles. Thus, the freezing process we see in the presence of an icosahedral seed is, in fact, homogeneous, and truly heterogeneous only in the presence of cubic seeds.

Figure 3 also includes some representative configurations of both crystallization regimes as well as the distributions $P(m_c)$ of the number m_c of particles on the seed surface that are in contact with particles belonging to the largest crystalline cluster. Hence, these distributions, shown for total cluster sizes 20–24, 50–54, and 500–504, quantify the fraction of the seed surface wetted by the crystal. For very small cluster sizes (20–24), the distribution of the number of contacts is double peaked, with one peak at $m_c = 0$ arising from the homogeneous nucleation events occurring away from the seed, and the other, broader peak corresponding to a partially covered seed. As the crystalline cluster grows, the homogeneous peak disappears and the other peak moves to larger numbers of wetted seed particles until the crystalline clusters become large enough to completely engulf the seed, which is the case for clusters larger than $\sim$55–65 particles. At this size, ideal clusters compatible with fcc (cuboctahedron with triangular faces, 55) and bcc (rhombic dodecahedron, 65) structures completely fill their third crystalline shell [25]. Thus, in both the fcc and bcc cases, the seed is completely wetted by the crystalline cluster long before it reaches critical size (see Sec. III C).

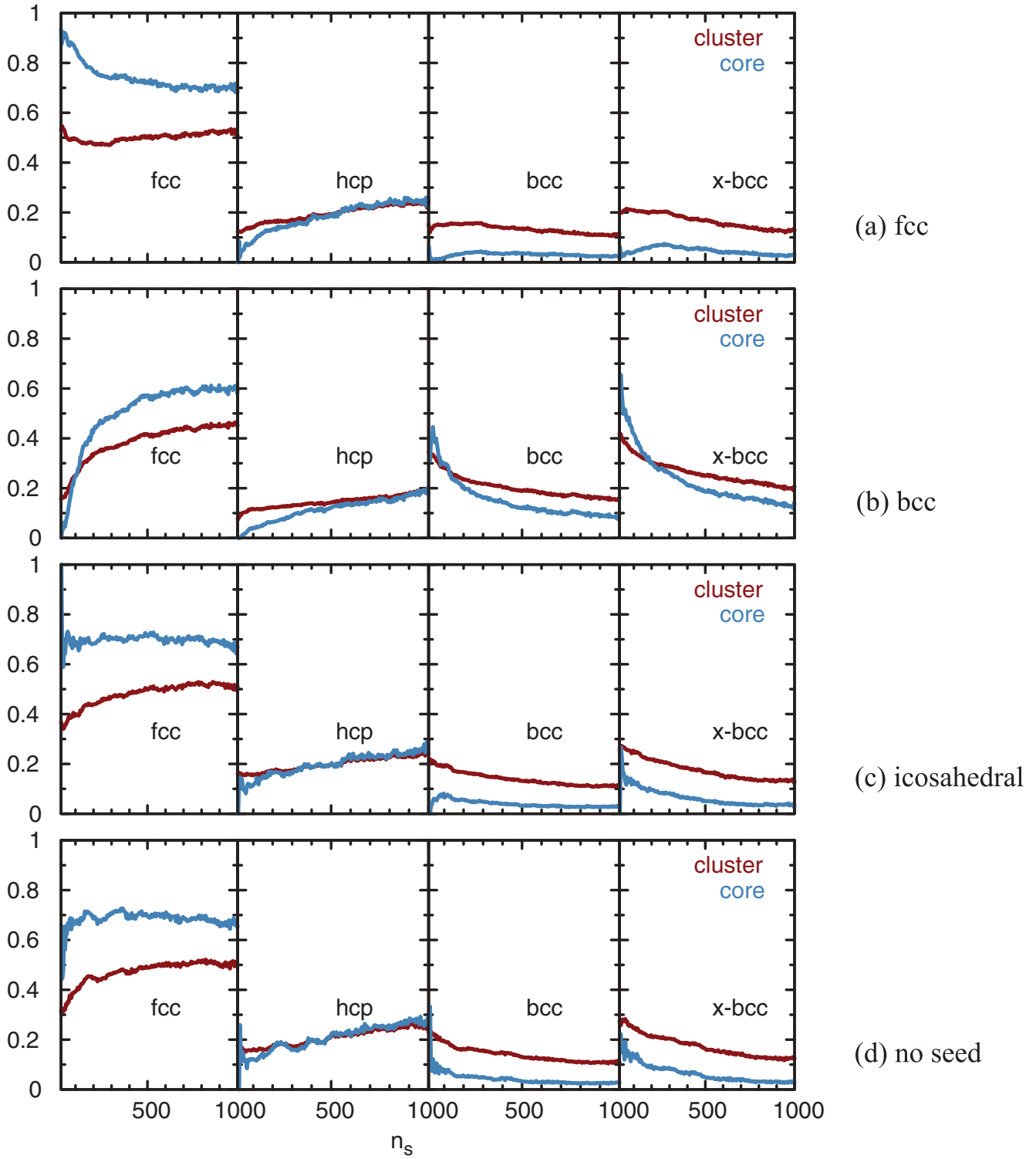

FIG. 2. (Color online) Fractions of crystalline structures in the largest cluster and its core in the presence of (a) fcc, (b) bcc, (c) icosahedral seeds, and in (d) a homogeneous system as a function of the largest cluster size, n_s. The fraction of particles with icosahedral structure is not shown as it is below 1% in all cases.

As can be inferred from Fig. 2, the structure of a crystal growing around a bcc seed changes from mostly bcc to predominantly fcc as the crystal grows. An interesting question is whether this transition from bcc to fcc occurs mainly close to the crystal-liquid interface moving outward during the cluster growth or also in the deeper regions of the crystal close to the seed. To address this issue we have monitored the structure evolution of the first layer around the bcc seed during the crystallization process. Crystalline particles in this first shell are predominantly of bcc type (approximately 2/3 of the particles) throughout the entire transformation with a slowly growing fraction of fcc particles. The fcc particles form at

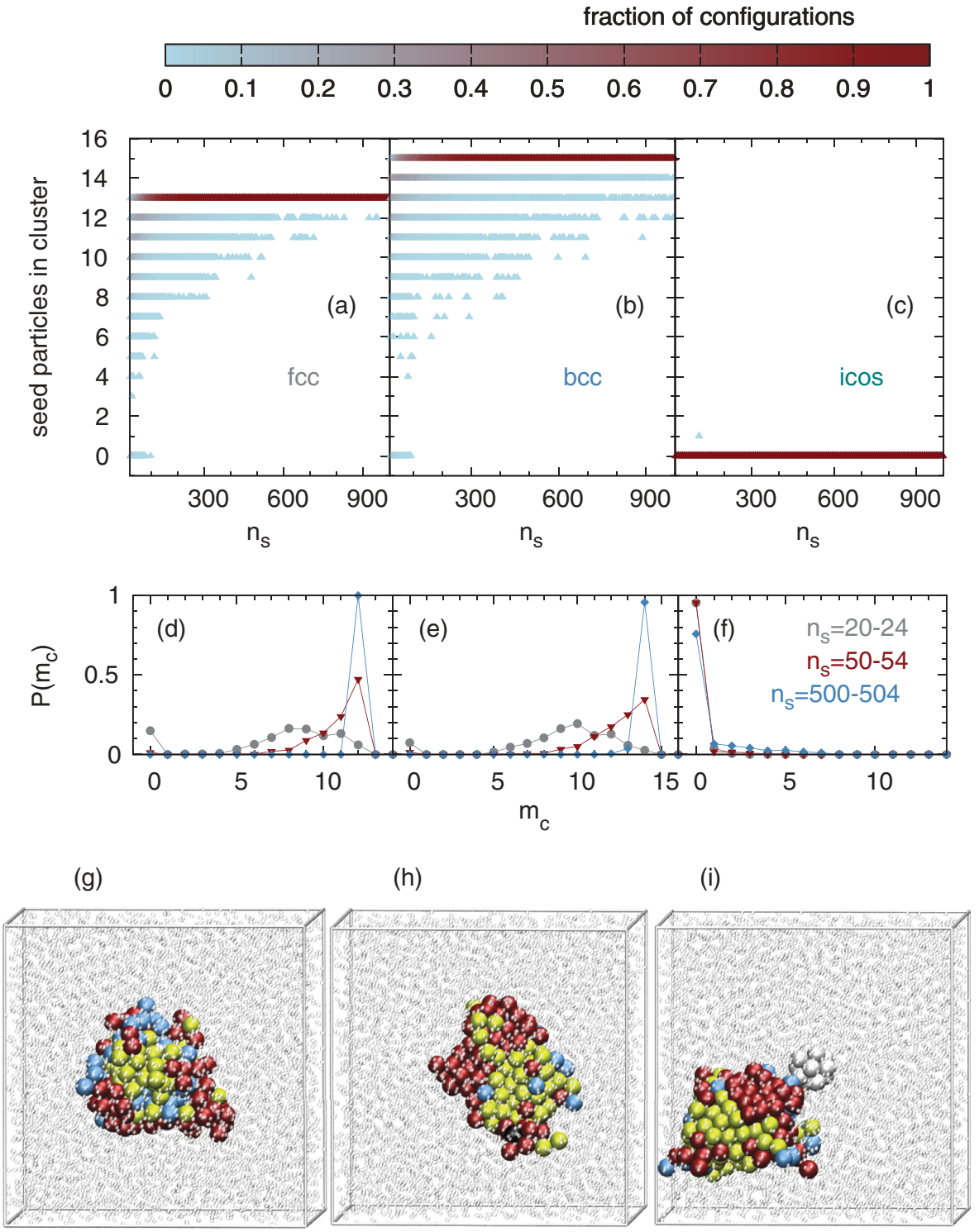

FIG. 3. (Color online) (a)–(c): Number of seed particles included into the largest cluster for (a) fcc, (b) bcc, and (c) icosahedral seeds, as a function of the largest cluster size, n_s. Symbols are colored according to the distribution of configurations along a particular cluster size. (d)–(f): Fractions $P(m_c)$ of configurations in which m_c of the particles on the seed surface are in contact with the crystalline cluster for (d) fcc, (e) bcc, (f) icosahedral seeds, and clusters with $n_s = 20$–24 (circles), 50–54 (triangles), and 500–504 (diamonds) particles. (g)–(i): Snapshots of critical clusters of sizes $n_s = 209$ (g), 226 (h), and 245 (i). Seed particles (only the icosahedral seed is not covered by cluster particles) are colored white, cluster particles are yellow (light gray) (fcc), blue (gray) (hcp), red (dark gray) (bcc), and black (icosahedral), and liquid particles are white and scaled in size for better view.

the expense of liquidlike particles, a few of which exist on the surface of the seed up to large cluster sizes. This finding can be explained by noting that although bcc seeds are mostly covered with crystalline particles, they tend to stay near the surface of the growing crystal, at which bcc particles occur with higher frequency. Seeds of fcc type, on the other hand, get

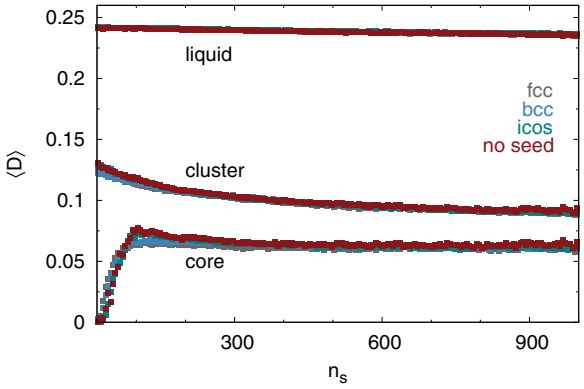

FIG. 4. (Color online) Average disorder parameters $\langle D \rangle$ according to Kawasaki and Onuki [22] for liquid, largest cluster and its core as a function of the largest cluster size, n_s.

buried deep in the interior of the crystal, where they eventually lose all the bcc particles that form in the initial growth stages.

Recently, Kawasaki and Onuki [22] proposed to use Steinhardt bond order parameters to measure disorder of the crystalline states, or the degree of deviation from hexagonal crystalline order. Here, we apply their analysis to our system. Intuitively, the presence of prestructured seeds, especially considering the increase of the fcc, respectively, bcc fractions in the small clusters, should result in more ordered structures. However, Fig. 4, which presents the measure of disorder of clusters, their cores, and the liquid part of the system, shows that the seeds are too small to have any noticeable effect. The disorder we find corresponds to the homogeneous case, in which the crystalline cluster is distinctively more ordered than liquid and less ordered than its core. The expected increase of order due to the presence of cubic seeds is only slightly noticeable for small cluster sizes.

C. Commitment analysis

To further characterize the transition mechanism, we carried out a commitment analysis of configurations selected from 30 crystallizing paths. From about 1300 configurations for every system, we initiated 100 trajectories to calculate the probability to end up in the crystalline state, or, in our case, with a largest cluster containing more than 1000 particles. The results presented in Fig. 5 show that the size of the critical clusters, i.e., the threshold size from which the clusters have the same probability to relax into the undercooled state or grow to fill the whole system, is distinctively changed by the presence of the seeds. The presence of an fcc seed shifts the distribution of critical cluster sizes to smaller values compared to the homogeneous case. As a result, the average critical cluster size is distinctively smaller: $\langle n_c^{\mathrm{fcc}} \rangle = 184$ vs $\langle n_c^{\mathrm{hom}} \rangle = 249$. In contrast, the presence of a bcc seed results in broadening of the critical cluster size distribution and its mean value is shifted to a large value, $\langle n_c^{\mathrm{bcc}} \rangle = 265$. The distribution of the critical cluster sizes in the presence of an icosahedrally ordered seed is comparatively narrow with a mean of $\langle n_c^{\mathrm{icos}} \rangle = 222$. Note, however, that the statistical inaccuracy in the estimate of the average size of the critical cluster is considerable due to the large variance of the distributions and the small sample

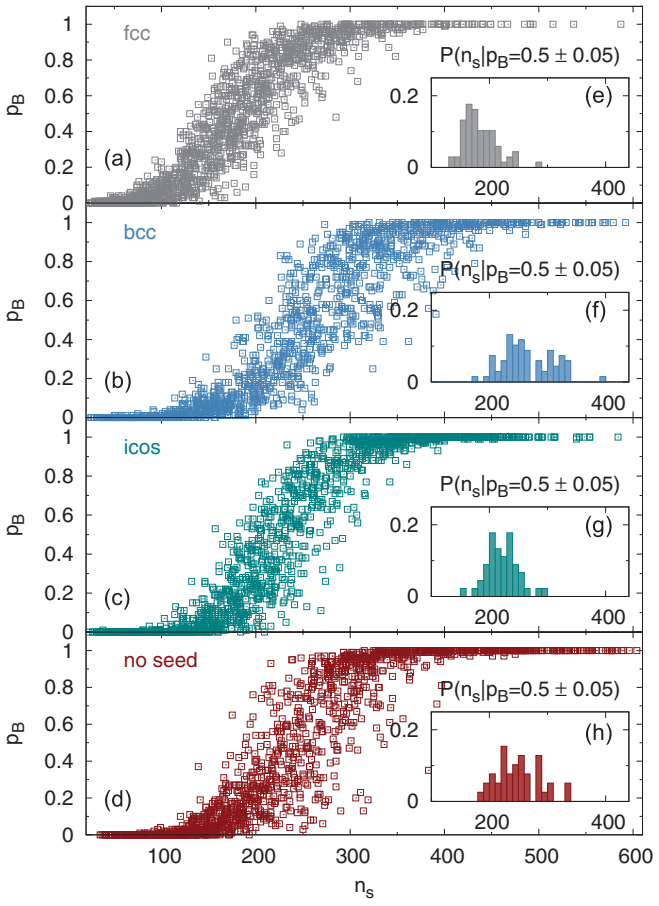

FIG. 5. (Color online) (a)–(d): Probabilities to reach a fully crystallized state as a function of the largest cluster size n_s, for the systems with (a) fcc, (b) bcc, (c) icosahedral, and (d) without any seed. (e)–(h): Size distributions of the respective critical clusters, identified from configurations that have a probability $p_B = 0.5 \pm 0.05$ to reach a crystalline state.

size, ranging from 40 to 70 configurations containing a critical cluster.

The average size of critical clusters also provides an explanation of the growth behavior of crystalline clusters shown in Fig. 1. The pace of growth, as quantified by the conditional crossing probability, is essentially the same for fcc and bcc seeds up to sizes for which the cluster is still subcritical in both cases. The fcc-seeded cluster, however, reaches criticality earlier and the crossing probability levels off at this size. The bcc-seeded crystals, on the other hand, need to grow further in order to reach critical sizes, at which a large fraction of the cluster has transformed from a bcc to an fcc structure. It is this later growth and transformation stage that causes the bcc seed to enhance the crystallization rate less than the fcc seed by about an order of magnitude.

In terms of the critical clusters, our findings confirm the results of the previous studies [23] on the homogeneous crystallization which state that not only the size but also the structures of crystallites are important to characterize the transition states. While the effects are too small for an exact analysis, the trend is that fcc structures found in small clusters decrease the critical cluster size relative to the homogeneous

crystallization, and the presence of bcc structures increases the critical cluster size.

IV. SUMMARY

In this work, we studied the kinetics and, in particular, the mechanism of crystallization near small crystalline seeds of various structures. Such heterogeneous nucleation processes caused by small foreign objects are ubiquitous in nature and also play a role in industrial processes. Using advanced computer simulation methods, we showed that the structure of the crystalline seeds determines the way heterogeneous crystallization proceeds. We consider seeds of the minimum size needed to define various structures and even for these tiny sizes we find crystallization rates that change by almost four orders of magnitude. While the presence of fcc- and bcc-structured seeds increases the rate relatively to the homogeneous case, the presence of an icosahedrally ordered seed has no effect on the crystallization transition.

The seeds we consider have a lattice spacing equal to that of the bulk crystal. We find that for fcc and bcc seeds crystallization occurs preferentially on the seed surface, while an icosahedrally ordered seed repels the solid clusters such that the nucleation process occurs away from the seed in the bulk undercooled liquid. In contrast, our previous work on the crystallization transition in the presence of squeezed seeds with lattice constant smaller than in equilibrium revealed a mixture of two crystallization regimes for an fcc as well as for an icosahedral seed, although the relative importance of the on-seed crystallization for an icosahedral seed, similar to the bulk crystallization in the presence of an fcc seed, was little. A similar effect has been observed previously for the crystallization of a hard sphere fluid near a size-mismatched sphere [9]. For foreign spheres of intermediate size, the seed clearly affected the transition pathway, but left the height of the nucleation barrier, and hence the nucleation rate unchanged.

The structures of small crystallites are strongly affected by the presence of seeds included into the crystalline cluster, both for fcc and bcc seeds. Seeds of bcc structure yield crystallites with a large fraction of bcc particles in the early stages of the crystallization process. Only later do these particles transform into the fcc structure as an instance of Ostwald's step rule. In contrast, fcc seeds lead to an initial depletion of bcc particles, bypassing the transient formation of a bcc phase. While the initial growth of crystallites occurs with the same rate for bcc and fcc seeds, crystallites growing on an fcc seed reach critical size earlier leading to a crystallization rate exceeding that of bcc-seeded crystallization by an order of magnitude. Both for fcc and bcc seeds, however, the structures observed in homogeneous nucleation are recovered as the clusters grow. Thus, the overall effects of the tiny seeds on the bulk crystalline phase are marginal, as expected. The icosahedral seed is not a part of the crystalline cluster, such that its structure is similar to that observed in the case of homogeneous crystallization.

Thus, we found that even tiny clusters can have a large effect on the crystallization transition depending on their particular structure. In future studies, we will investigate how the size of the prestructured seeds influences the crystallization transition. While small icosahedral seeds do not affect the crystallization, large icosahedral structures may enhance the nucleation rate due to the fcc (111) surfaces they expose to the supercooled liquid. Due to their geometric incompatibility with the target structure, a growing crystal might separate from the seed making it available for another nucleation event. Similar interplays of surface structure and morphology may also be possible for seeds with other crystal structures. Another interesting question concerns the minimum cluster size needed to induce spontaneous barrierless growth. It is clear that crystals will grow on the seeds larger than the critical cluster size, but the presence of prestructured seeds changes the critical cluster size such that only further simulations can answer this question.

ACKNOWLEDGMENTS

The computational results presented have been achieved, in part, using the Vienna Scientific Cluster (VSC). We acknowledge financial support from the Austrian Science Fund (FWF) within the SFB ViCoM (Grant No. F41) as well as Project No. P 24681-N20.

[1] W. Ostwald, Z. Phys. Chem. **22**, 289 (1897).
[2] M. Hermes, E. C. M. Vermolen, M. E. Leunissen, D. L. J. Vossen, P. D. J. van Oostrum, M. Dijkstra, and A. van Blaaderen, Soft Matter **7**, 4623 (2011).
[3] H. J. Schöpe and P. Wette, Phys. Rev. E **83**, 051405 (2011).
[4] V. W. A. de Villeneuve, D. Verboekend, R. P. A. Dullens, D. G. A. L. Aarts, W. K. Kegel, and H. N. W. Lekkerkerker, J. Phys.: Condens. Matter **17**, S3371 (2005).
[5] A. Cacciuto, S. Auer, and D. Frenkel, Nature (London) **428**, 404 (2004).
[6] R. P. Sear, J. Phys. Chem. B **110**, 4985 (2006).
[7] M. Heni and H. Löwen, Phys. Rev. Lett. **85**, 3668 (2000).
[8] M. Heni and H. Löwen, J. Phys.: Condens. Matter **13**, 4675 (2001).
[9] A. Cacciuto and D. Frenkel, Phys. Rev. E **72**, 041604 (2005).
[10] H. Wang, H. Gould, and W. Klein, Phys. Rev. E **76**, 031604 (2007).
[11] A. R. Browning, M. F. Doherty, and G. H. Fredrickson, Phys. Rev. E **77**, 041604 (2008).
[12] S. van Teeffelen, C. N. Likos, and H. Löwen, Phys. Rev. Lett. **100**, 108302 (2008).
[13] W.-S. Xu, Z.-Y. Sun, and L.-J. An, J. Chem. Phys. **132**, 144506 (2010).
[14] G. I. Tóth, G. Tegze, T. Pusztai, and L. Gránásy, Phys. Rev. Lett. **108**, 025502 (2012).
[15] S. Jungblut and C. Dellago, Europhys. Lett. **96**, 56006 (2011).
[16] H. C. Andersen, J. Chem. Phys. **72**, 2384 (1980).
[17] S. Auer and D. Frenkel, J. Chem. Phys. **120**, 3015 (2004).

[18] P. J. Steinhardt, D. R. Nelson, and M. Ronchetti, Phys. Rev. B **28**, 784 (1983).
[19] W. Lechner and C. Dellago, J. Chem. Phys. **129**, 114707 (2008).
[20] S. Jungblut and C. Dellago, J. Chem. Phys. **134**, 104501 (2011).
[21] H. Eshet, F. Bruneval, and M. Parrinello, J. Chem. Phys. **129**, 026101 (2008).
[22] T. Kawasaki and A. Onuki, J. Chem. Phys. **135**, 174109 (2011).
[23] D. Moroni, P. R. ten Wolde, and P. G. Bolhuis, Phys. Rev. Lett. **94**, 235703 (2005).
[24] I. N. Stranski and D. Totomanow, Z. Phys. Chem. **163**, 399 (1933).
[25] T. Martin, Phys. Rep. **273**, 199 (1996).